Effects of acidic-basic properties on catalytic activity for the oxidative dehydrogenation of isobutane on calcium phosphates, doped and undoped with chromium

Takuya EHIRO[1], Hisanobu MISU[1], Shinya NITTA[1], Yuzo BABA[2], Masahiro KATOH[2], Yuuki KATOU[3], Wataru NINOMIYA[3] and Shigeru SUGIYAMA[2,4]*

[1]*Department of Chemical Science and Technology, Tokushima University, Minamijosanjima, Tokushima-shi, Tokushima 770-8506, Japan*

[2]*Department of Applied Chemistry, Graduate School of Science and Technology, Tokushima University, Minamijosanjima, Tokushima-shi, Tokushima 770-8506, Japan*

[3]*Otake Research Laboratories, Mitsubishi Rayon Co. Ltd., 20-1, Miyuki-cho, Otake-shi, Hiroshima 739-0693, Japan*

[4]*Department of Resource Circulation Engineering, Center for Frontier Research of Engineering, Tokushima University, Minamijosanjima, Tokushima-shi, Tokushima 770-8506, Japan*

Keywords: Oxidative dehydrogenation, Isobutane, Calcium hydroxyapatite, Acidic property, Basic property

Abstract

Catalytic activities of calcium hydroxyapatite (HAp) and β-type tricalcium phosphate (β-TCP) were examined for use in the oxidative dehydrogenation (ODH) of isobutane. β-TCP was catalytically inactive for the ODH of isobutane, but stoichiometric HAp afforded a high isobutene yield (5.6%). The isobutane conversion and isobutene selectivity of HAp depended on the atomic ratio of Ca/P. HAp with Ca/P = 1.67 showed the highest isobutene selectivity and isobutene yield among the HAp catalysts with different Ca/P ratios. The characterization of the acidic-basic properties showed that these properties affect the catalytic performance of HAp, and that its basicity is necessary for high catalytic activity. To improve the catalytic activities of calcium phosphates, they were impregnated with Cr. Despite a much lower surface area for β-TCP, Cr-impregnated β-TCP showed a higher isobutene yield (up to 8.4%) than that of Cr-impregnated HAp. The results of the XPS measurement showed that the Cr^{3+} species on calcium phosphates, owing to basicity, worked as active sites in the ODH of isobutane.

Introduction

Methyl methacrylate (MMA) is a chemical in high demand, mainly for the production of poly(methyl methacrylate) (PMMA) acrylic plastics and methyl methacrylate-butadiene-styrene (MBS) co-polymers. Various routes to produce MMA have been proposed, developed, and put into operation (Ninomiya, 2014). As a typical and classic method for the production of MMA, acetone cyanohydrin (ACH) processing is widely used. In ACH processing, acetone and hydrogen cyanide, produced in the petrochemical industry as by-products of phenol and acrylonitrile, respectively, are employed as raw materials. As a result, ACH processing is strongly influenced by the production of these raw materials; moreover, toxicity of hydrogen cyanide is also a serious problem. In order to overcome these problems, we focused on two processes for the production of MMA: C4 direct oxidation and C4 oxidative esterification. In these processes, isobutene is used as the raw material. However, isobutene is currently produced mainly via naphtha cracking, which consumes a huge amount of energy. Hence, we have investigated the oxidative dehydrogenation (ODH) of isobutane to produce isobutene (and MMA) efficiently. In addition to the production of MMA, isobutene is also used for the production of gasoline additives, butyl rubbers, and so on.

E-mail address of corresponding author: sugiyama@tokushima-u.ac.jp*

To produce isobutene efficiently, the dehydrogenation (DH) of isobutane, which is directly produced from petroleum refining in an inefficient process, has been investigated (Ohta *et al*., 2004; Korhonen *et al*., 2007). However, the DH of isobutane requires a higher reaction temperature than the ODH of isobutane due to its endothermic reaction. In the present study, we used oxygen as a reactant gas because it renders the reaction exothermic. Moreover, oxygen can render a reaction field unfavorable for coke deposition and it can prevent rapid deactivation of a catalyst, as confirmed in the DH of isobutane.

For a heterogeneous reaction, various factors affect the catalytic activity, such as particle size, surface area, particle shape, and reaction conditions. More interestingly, the acidic, basic, and redox properties of catalysts are known to affect their catalytic performances for the ODH of isobutane (Wang *et al*., 2009; Zhang *et al*., 2009; Sugiyama *et al*., 2015). Hence, calcium hydroxyapatite (HAp) was used for the ODH of isobutane in the present study since HAp shows acidic-basic properties. In addition, various types of anions and cations can be exchanged with PO_4^{3-} and Ca^{2+} that make HAp (Matsuura *et al*., 2014). Also, the Ca/P ratios of HAp vary from 1.50 to 1.67. It is known that stoichiometoric HAp with Ca/P = 1.67 shows acidic-basic properties. On the contrary, as the Ca/P ratio decreases from 1.67 to 1.50, the number of acidic

sites increases and that of basic sites decreases. Hence, HAp was used in the present study to investigate the effects of its acidic-basic properties on its catalytic activity by changing its Ca/P ratio. For comparison with HAp, β-type tricalcium phosphate (β-TCP), which shows weak basicity, was also examined as a catalyst for the ODH of isobutane. Moreover, stoichiometric HAp and β-TCP were impregnated with Cr species to improve their catalytic activities, since Cr-containing catalysts show high catalytic activities for the ODH of isobutane (Wang *et al*., 2009; Zhang *et al*., 2009; Sugiyama *et al*., 2015; Ehiro *et al*., 2015; Ehiro *et al*., 2016a).

1. Experimental

1.1 Catalyst preparation

HAp was prepared as follows. First, 39.5 g (165 mmol) of $Ca(NO_3)_2$ (Wako Pure Chemical Industries, Ltd.) and 13.2 g (99.0 mmol) of $(NH_4)_2HPO_4$ (Wako Pure Chemical Industries, Ltd.) were dissolved in 150 and 250 mL of distilled water, respectively, as reported by Hayek and Newesely (1963). Second, the pH values of $Ca(NO_3)_2$ aq. and $(NH_4)_2HPO_4$ aq. were adjusted to 11.25 and 10.25, respectively, by adding NH_3 aq. (Wako Pure Chemical Industries, Ltd.). Third, the above pH-adjusted solutions were diluted with distilled water to 300 and 400 mL, respectively. After dilution, the above two solutions were mixed quickly with vigorous stirring. Then, the resulting white precipitate was filtered, washed with distilled water, and dried at 353 K. Finally, HAp was obtained by calcination of the dried sample at 773 K for 3 h. In addition to HAp prepared from a stoichiometric solution with Ca/P = 1.67, Ca-deficient HAp catalysts were also prepared from nonstoichiometric solutions with Ca/P ratios = 1.50, 1.55, and 1.62 in order to compare them with the stoichiometric HAp. The HAp prepared from precursor solutions with Ca/P = x are hereafter referred to as HAp(x). After the preparations of HAp catalysts from the precursors with different Ca/P ratios, the amounts of Ca and P of HAp(1.50) and HAp(1.67) were analyzed via ICP-AES (SPS3520UV, SII Nanotechnology Inc.), and the Ca/P ratios were calculated to be 1.53 and 1.66, showing that HAp with different Ca/P ratios can be prepared as expected. The β-TCP used in the present study was purchased from Nakarai Tesque Inc. Both the stoichiometric HAp prepared from Ca/P = 1.67 and β-TCP were used not only as the catalyst but also as support for the impregnation of Cr. To improve the catalytic activities of HAp and β-TCP, Cr impregnation was conducted via a conventional impregnation method using an aqueous solution of $Cr(NO_3)_3$ (Sigma-Aldrich Japan) as a Cr source. In the present study, the Cr content was adjusted to 1.5, 3.5, 5.0, or 7.0 wt%.

1.2 Catalyst characterization

The structural properties of the catalysts were analyzed via X-ray diffraction (XRD; RINT 2500X, Rigaku Co.), N_2 adsorption-desorption measurement (BELSORP-max12, MicrotracBEL), and scanning electron microscopy (SEM; JSM-6510A, JEOL ltd.). The powder XRD patterns of the catalysts were obtained using monochromatized Cu Kα radiation (40 kV, 40 mA). Before the N_2 adsorption-desorption measurement at 77 K, the catalysts were pretreated at 473 K for 5 h in a vacuum. The BET surface area was calculated from the obtained isotherm.

The acidic and basic properties of the catalysts were characterized via NH_3 and CO_2 temperature-programmed desorption (TPD; BELCAT II, MicrotracBEL), respectively. In NH_3- and CO_2-TPD measurements, a catalyst (50 mg) was loaded into a quartz tube. Prior to each run, a catalyst was pretreated under 50 sccm of He flow at 773 K for 1 h, and then cooled to 373 or 343 K in NH_3- or CO_2-TPD, respectively. After these temperatures were maintained for 10 min, the catalyst was treated with 50 sccm of 5% NH_3/He or 5% CO_2/He gas for 30 min. After the treatments, the catalyst was again kept under a He flow (50.0 sccm) for 15 min. The catalyst was then heated from 373 or 343 K to 883 K at 10 K/min by flowing 30 sccm of He gas. Desorbed NH_3 or CO_2 from the catalyst was monitored using a quadrupole mass spectrometer (BELMass, MicrotracBEL). A fragment peak at m/e = 16 or 44 was used to monitor the desorbed NH_3 or CO_2, respectively.

The redox properties and chemical states of the Cr species were evaluated via X-ray photoelectron spectroscopy (XPS; PHI-5000VersaProbe II, ULVAC-PHI Inc.), X-ray absorption fine structure (XAFS) measurement, H_2 temperature-programmed reduction (TPR; BELCAT-A, MicrotracBEL) technique, and Raman spectroscopy (SH0056, Renishaw via Raman microscopy). The XPS spectra of the catalysts were calibrated based on the C 1s peak at 285.0 eV. Analysis of the XAFS near the Cr-*K* edge was performed via synchrotron radiation at the beam-line NW9A station of the Photon Factory in the High Energy Accelerator Research Organization (Tsukuba, Japan) with a storage ring current of ~400 mA (2.5 GeV). The X-ray was monochromatized with Si(111). The absorption spectra were observed using ionization chambers in the transmission mode. The photon energy was scanned from 5,589 to 6,783 eV for the Cr-*K* edge. H_2-TPR measurement was carried out by flowing 40 sccm of 5% H_2/Ar gas from 373 to 1,073 K at a rate of 10 K/min. The amount of H_2 consumption was determined via TCD. Water in the produced gas was trapped with a molecular sieve, 13X, before any gas had passed through the TCD. Each catalyst (50 mg) was exposed to a pretreatment of 50 sccm of Ar gas flow at 773 K for 1 h before flowing 40 sccm 5% H_2/Ar gas. Raman

spectra of the Cr-containing samples were recorded by using a laser excitation wavelength of 532 nm.

1.3 Catalytic activity testing

The catalytic activity tests were carried out in a fixed-bed continuous flow reactor at atmospheric pressure. Each catalyst (0.25 g) was pelletized and sieved to 0.85–1.70 mm. They were fixed with quartz wool and pretreated with 12.5 mL/min of O_2 gas flow at 723 K for 1 h. After the pretreatment, catalytic activity tests were started by flowing 15 mL/min of a mixed gas of helium, isobutane, and oxygen to the reactor. Their partial pressures were adjusted to P(He) = 74.6 kPa, P(i-C_4H_{10}) = 14.4 kPa, and P(O_2) = 12.3 kPa, respectively. These reaction conditions were used unless otherwise stated. Under these conditions, a homogeneous gas phase reaction was not observed. All catalysts showed stable activities up to 6 h on-stream. The reaction was monitored using an online gas chromatograph (GC-8APT, Shimadzu Corp.) equipped with a TCD. A Molecular Sieve 5A (MS 5A, 0.2 m×Φ3 mm) for O_2, CH_4, and CO and a Hayesep R (2.0 m×Φ3 mm) for CO_2, C2, C3, and C4 products were used as the columns. The carbon balance between the reactant and the products was within ±5%. The product selectivity and isobutane conversion were calculated on a carbon basis.

In addition to the ODH of isobutane, an ethanol conversion reaction was also conducted over the catalysts. A Ca-deficient HAp is known to convert ethanol to ethylene over its acid sites, although stoichiometric HAp converts ethanol to acetaldehyde or 1-butanol over its base sites (Tsuchida *et al*., 2008). Therefore, the obtained product selectivities were used to evaluate the acidic-basic properties of catalysts. A catalyst (0.15 g, 0.85–1.70 mm) was loaded into a fixed bed continuous reactor. Each catalyst was pretreated with 25 mL/min of oxygen at 673 K. Then, the reaction was started by flowing 30 mL/min of He gas and 1.7 mL/h of ethanol liquid at 673 or 773 K. Ethanol conversion and product selectivities were calculated on a carbon basis by using a capillary gas chromatograph (GC2010, Shimadzu Corp.).

2. Results and Discussion

2.1 Physical properties

Fig. 1 shows the XRD patterns of the catalysts doped and undoped with Cr. The structures of HAp(1.67) and β-TCP remained unchanged after Cr impregnation. In addition, XRD patterns similar to those of stoichiometric HAp(1.67) were detected for HAp catalysts with different Ca/P ratios (not shown). Peaks due to crystalline α-Cr_2O_3 (JCPDS 381479) are shown in Fig. 1. These peaks became stronger as the Cr content was increased. **Table 1** shows the physical properties of the catalysts, doped and undoped with Cr, obtained via nitrogen adsorption-desorption

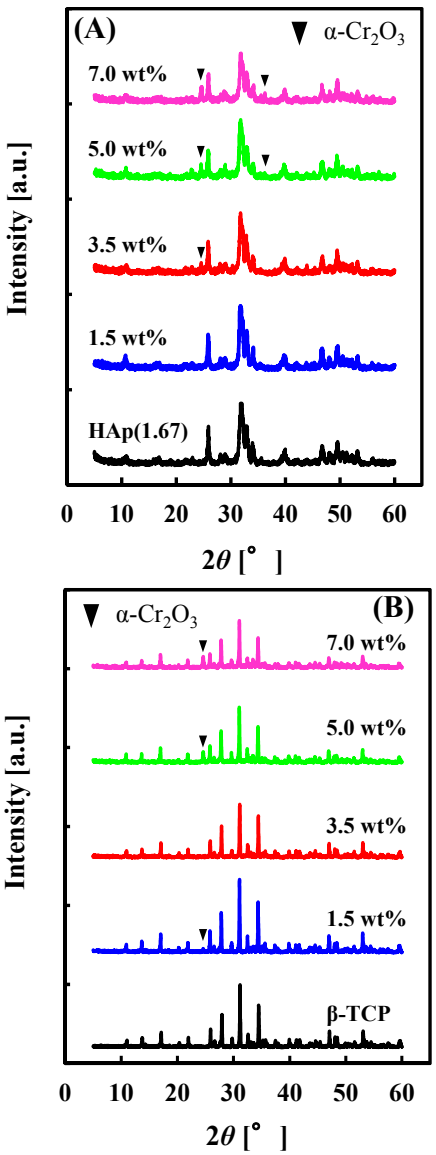

Fig. 1 XRD patterns of (A) undoped and Cr-doped stoichiometric HAp(1.67) catalysts and (B) undoped and Cr-doped β-TCP catalysts.

Table 1 Physical properties of calcium phosphate catalysts, doped and undoped with Cr used in the present study.

Catalyst	Cr content [wt%]	BET Surface area [m^2/g]
HAp(1.50)	0	75.6
HAp(1.55)	0	66.2
HAp(1.62)	0	64.1
HAp(1.67)	0	63.3
Cr/HAp	1.5	61.9
	3.5	53.5
	5.0	61.8
	7.0	52.5
β-TCP	0	1.8
Cr/β-TCP	1.5	2.1
	3.5	2.5
	5.0	3.3
	7.0	4.1

measurements. As reported previously (Tsuchida *et al*., 2008), the BET surface area of β-TCP was much lower than that of HAp(1.67). Also, the BET surface areas of Ca-deficient HAp catalysts were confirmed as similar to that of HAp(1.67) (Table 1). Cr impregnation did not significantly affect the BET surface areas of HAp or β-TCP.

Fig. 2 shows the SEM images of HAp(1.67), HAp(1.50), and β-TCP. It was evident that the stoichiometric HAp(1.67) was roughly spherical (Fig. 2 (a)), while the β-TCP particles were rectangular and nodular (Fig. 2 (c)). The stoichiometric HAp(1.67) differed from the Ca-deficient HAp(1.50) in both shape and size (Figs. 2 (a) and (b)). HAp(1.50) particle surfaces looked roughly flat, and were prominently seen. However, the majority of HAp(1.67) particles had rough surfaces and looked less crystalline than those of HAp(1.50), although their XRD patterns were similar. Due to the lower crystallinity of HAp(1.67), it may be possible to break its crystals into small and rough particles. For the above reason, roughly spherical particles may have been prominently observed for HAp(1.67). Since the HAp crystal has two different surfaces (a- and c-planes), exposed ions on the surfaces of HAp(1.50) and HAp(1.67) particles would be different. Hence, HAp(1.50) and HAp(1.67) catalysts can be expected to show different catalytic activities for the ODH of isobutane.

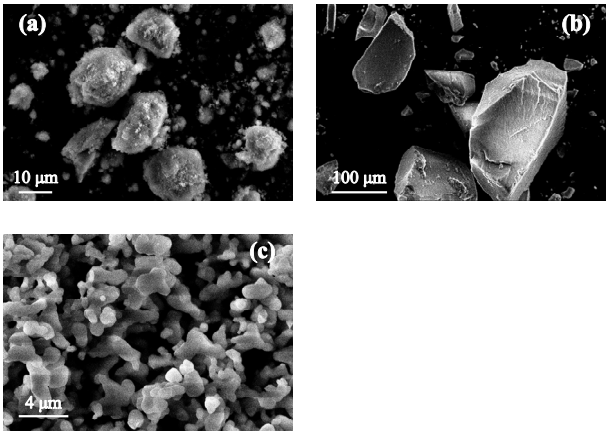

Fig. 2 SEM images of (a) HAp(1.67), (b) HAp(1.50), and (c) β-TCP.

2.2 Catalytic activities of HAp and β-TCP catalysts for the ODH of isobutane

Table 2 shows the catalytic activities of the undoped HAp and β-TCP catalysts for the ODH of isobutane at 6.0 h on-stream. Among the undoped catalysts, stoichiometric HAp(1.67) showed the best catalytic performance. The catalytic activity for the ODH of isobutane was believed to be related to the acidic-basic properties. The correlation between the catalytic activity and acidic-basic properties was discussed previously in relation to lactic acid conversion on HAp (Matsuura *et al*., 2014).

Table 2 Catalytic activities of β-TCP and undoped HAp catalysts for the ODH of isobutane at 6.0 h on-stream.

Catalyst	Conversion [%]	Selectivity [%]		Yield [%]
	i-C_4H_{10}	COx	i-C_4H_8	i-C_4H_8
β-TCP	2.5	76.1	20.0	0.5
HAp(1.50)	7.4	77.0	19.5	1.4
HAp(1.55)	15.0	82.9	10.4	1.6
HAp(1.62)	13.6	74.2	17.6	2.4
HAp(1.67)	13.9	57.6	40.4	5.6

2.3 Acidic-basic properties of HAp and β-TCP catalysts

Fig. 3 shows the NH_3- and CO_2-TPD spectra of β-TCP and HAp catalysts. The numbers of acidic and basic sites were calculated from the desorption peaks of the NH_3- and CO_2-TPD spectra (**Table 3**). As shown in Fig. 3, the stoichiometric HAp showed acidic-basic properties and β-TCP showed weak basicity (Table 3). The basicity of the stoichiometric HAp decreased as its Ca/P ratio decreased. On the contrary, it is easy to see that the desorption peaks of Ca-deficient HAp catalysts were slightly shifted to a higher-temperature region (Fig. 3 (A)). This means that its acidity was strengthened slightly as its Ca/P ratio decreased, as reported previously (Tsuchida *et al*., 2008).

The acidic-basic properties of the catalysts were also evaluated via ethanol conversion reactions. **Table 4** and **Fig. 4** show the results of the ethanol conversion reaction at 3.25 h on-stream. The number and strength of acid and base sites can determine the reaction mechanism of ethanol conversion and its products. As proposed previously (Angelici *et al*., 2015), acetaldehyde can be produced through the E1cB mechanism that requires cooperative action between

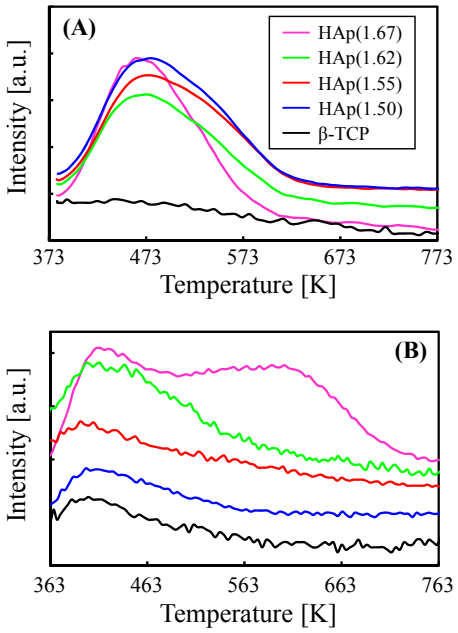

Fig. 3 (A) NH_3-TPD and (B) CO_2-TPD spectra of β-TCP, HAp(1.50), HAp(1.55), HAp(1.62), and HAp(1.67).

Table 3 BET surface area and the amounts of acid and base sites of HAp and β-TCP catalysts.

Catalyst	BET surface area [m^2/g]	Density [μmol/m^2] of	
		acid sites	base sites
β-TCP	1.8	—	0.56
HAp(1.50)	75.6	1.58	0.11
HAp(1.55)	66.2	1.72	0.22
HAp(1.62)	64.1	1.51	0.28
HAp(1.67)	63.3	1.97	0.97

Table 4 Results of ethanol conversion reaction over β-TCP at 773 K and undoped HAp at 673 K and 3.25 h on-stream.

Catalyst	Ethanol conversion [%]	Ethylene selectivity [%]	Acetaldehyde+1-butanol selectivity [%]
β-TCP[a)]	15.5	2.9	66.6
HAp(1.50)	6.2	79.7	13.2
HAp(1.55)	6.2	81.0	7.6
HAp(1.62)	7.5	69.7	14.6
HAp(1.67)	5.9	30.0	53.0

a) The reaction was conducted at 773 K because ethanol conversion of β-TCP at 673 K was too low (≦0.5%).

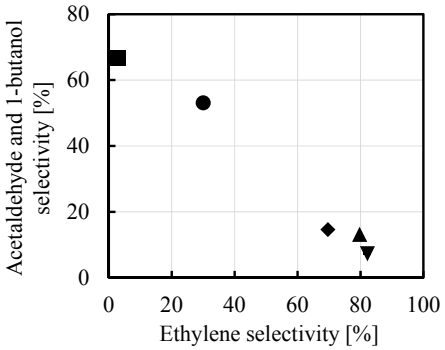

Fig. 4 Acetaldehyde and 1-butanol selectivity versus ethylene selectivity on β-TCP (■) at 773 K, HAp(1.50) (▲), HAp(1.55) (▼), HAp(1.62) (◆), and HAp(1.67) (●) at 673 K and 3.25 h on-stream.

acidic and basic sites. One of two neighboring aldehyde intermediates can be decomposed to an enolate (carbanion intermediate), which reacts with the other aldehyde intermediate to form aldol (aldol condensation). Unsaturated aldehyde is then generated by dehydration of the aldol, and, finally, 1-butanol is synthesized via hydrogenation of the unsaturated aldehyde (hydride reduction), taking up hydrogen generated by dissociative adsorption during the production of acetaldehyde and aldol (Tsuchida *et al*., 2008). Ethylene can be produced through E1, E2, and E1cB mechanisms (Angelici *et al*., 2015). Only acid sites were involved in the dehydration of ethanol via the E1 route. E2 and E1cB routes require cooperative action between acidic and basic sites. However, to dehydrate ethanol through the E1cB mechanism, stronger basic sites are required (Angelici *et al*., 2015). As mentioned above, the acidic sites on HAp promoted ethanol dehydration to produce ethylene (Fajardo *et al*., 2008; Tsuchida *et al*., 2008). Additionally, the basic sites on HAp have been used to catalyze the ethanol conversion reaction to produce mainly acetaldehyde and 1-butanol (Fajardo *et al*., 2008; Tsuchida *et al*., 2008). Hence, the lower-right side of the plot in Fig. 4 shows a catalyst with more acidic sites, while the upper-left of the plot in Fig. 4 shows a catalyst with more basic sites. For comparison with HAp catalysts, β-TCP, which shows weak basicity, was investigated for ethanol conversion at 673 K. However, its ethanol conversion was less than 0.5%. Therefore, to obtain a clearer result, only β-TCP was tested at 773 K. Although the higher temperature activates and converts products as well as ethanol, the obtained selectivity was compared with those of HAp catalysts. Basicity was mainly confirmed for β-TCP and HAp(1.67), while acidity was mainly observed for Ca-deficient HAp catalysts. These results were supported by NH_3- and CO_2-TPD measurements (Fig. 3 and Table 3). Ethanol conversions of HAp catalysts with different Ca/P ratios were slightly different (Table 4). Since HAp catalysts with different Ca/P ratios showed similar behaviors during ethanol conversion, with 10.0% and 20.0% ethanol conversion (Tsuchida *et al*., 2008), the differences in the total ethanol conversions were disregarded in the present study.

2.4 Acidic properties of Cr-doped catalysts

Acidic sites on mesoporous silica catalysts have been used to catalyze the ODH of isobutane (Ehiro *et al*., 2016b). However, the catalytic activity of Ca-deficient HAp gradually decreased as its Ca/P ratio and basicity decreased. It was significant that a slight difference in the acid strength of a HAp catalyst was insufficient to catalyze the ODH of isobutane. The best catalytic performance of stoichiometric HAp(1.67) implied that the basic sites on a HAp catalyst were essential in order to catalyze the ODH of isobutane. It was possible that both acidic and basic sites on HAp(1.67) catalyzed the ODH of isobutane synergistically, as has been discussed previously for lactic acid conversion (Matsuura *et al*., 2014). The crystal system of HAp is hexagonal and has two types of crystal planes with two opposite charges: positive on the a-planes and negative on the c-planes (Zhuang *et al*., 2012). Calcium ions (basic sites), phosphoric acids and hydroxyl groups (acidic sites) are known to be exposed mainly on the a-planes and c-planes, respectively (Zhuang and Aizawa, 2013). As confirmed via SEM, however, the stoichiometric HAp(1.67) was roughly spherical (Fig. 2 (a)). Based on this SEM image, it was estimated that the acidic and basic sites on the stoichiometric HAp(1.67) were closer than those on Ca-deficient HAp(1.50) (Figs. 2 (a) and (b)). Hence, it would be easier for acidic and basic sites to catalyze the ODH of isobutane synergistically.

As mentioned above, the solid acidity of a catalyst could play a crucial role in determining its catalytic activity for the ODH of isobutane. Therefore, the acidic properties of stoichiometric HAp, both doped and undoped with Cr, were also examined using NH_3-TPD (**Fig. 5**). Although it is known that a mixture of some

materials such as metal oxides could enhance the solid acidity of a composite material, the acidity of Cr-doped HAp decreased as the Cr content increased. This result indicated that the acidic sites of stoichiometric HAp(1.67) were covered by chromium oxides such as crystalline α-Cr_2O_3, which is confirmed in Fig. 1 (A). Solid acidity of crystalline α-Cr_2O_3 could not be confirmed via NH_3-TPD. Also, no improvement in solid acidity was observed via NH_3-TPD for the Cr-doped β-TCP catalysts. (not shown).

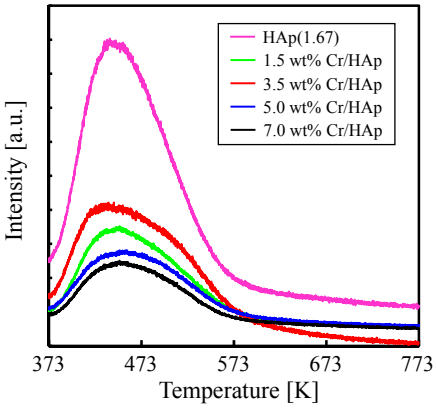

Fig. 5 NH_3-TPD spectra of stoichiometric HAp, doped and undoped with Cr.

2.5 Catalytic activities of the Cr-doped catalysts

Although stoichiometric HAp(1.67) catalyzed the ODH of isobutane (Table 2), a further improvement in the catalytic activity was required. Therefore, Cr impregnation was conducted using $Cr(NO_3)_3$ aq., because Cr-containing catalysts have shown relatively high catalytic activities for the ODH of isobutane (Wang *et al*., 2009; Zhang *et al*., 2009; Sugiyama *et al*., 2015; Ehiro *et al*., 2015, 2016a). Although β-TCP was much less catalytically active than HAp(1.67) (Table 2), Cr-doped β-TCP was more catalytically active than Cr-doped HAp(1.67) (**Table 5**).

Moreover, the effects of the feed ratio (i-C_4H_{10}/O_2) on the catalytic activity of Cr-doped HAp(1.67) and β-TCP were investigated (**Table 6**). For both catalysts, isobutane conversion together with CO_2 selectivity increased, while isobutene selectivity decreased as the i-C_4H_{10}/O_2 ratio decreased. This result may be reasonable since an oxygen-rich atmosphere promotes isobutane conversion and side reactions such as isobutene to COx. Finally, the isobutene yields of both catalysts were almost constant at any i-C_4H_{10}/O_2 ratio (Table 6).

Table 5 Catalytic activities at 723 K and 6.0 h on-stream of HAp(1.67) and β-TCP, both doped and undoped with Cr.

Catalyst	Cr content [wt%]	Conversion [%]	Selectivity [%]		Yield [%]
		i-C_4H_{10}	COx	i-C_4H_8	i-C_4H_8
HAp(1.67)	-	13.9	57.6	40.4	5.6
Cr/HAp	1.5	23.2	71.2	27.2	6.3
	3.5	20.9	66.2	32.4	6.8
	5.0	21.8	66.5	32.5	7.1
	7.0	24.4	68.0	31.1	7.6
β-TCP	-	2.5	76.1	20.0	0.5
Cr/β-TCP	1.5	22.5	63.1	33.5	7.5
	3.5	21.7	64.7	33.5	7.3
	5.0	22.4	63.7	34.8	7.8
	7.0	23.9	63.5	35.3	8.4

Table 6 Effects of i-C_4H_{10}/O_2 ratio on catalytic activities at 723 K and 6.0 h on-stream of HAp(1.67) and β-TCP, both doped and undoped with Cr.

Catalyst	i-C_4H_{10}/O_2 [-]	Conversion [%]	Selectivity [%]		Yield [%]
		i-C_4H_{10}	COx	i-C_4H_8	i-C_4H_8
3.5 wt% Cr/HAp	1.2	20.9	66.2	32.4	6.8
	0.6	33.7	77.0	21.7	7.3
	0.4	44.8	81.7	15.9	7.1
3.5 wt% Cr/β-TCP	1.2	21.7	64.7	33.5	7.3
	0.6	33.3	75.4	23.3	7.8
	0.4	49.1	82.2	15.8	7.8

2.6 Chemical states of the Cr species on the Cr-doped catalysts

In order to investigate catalytically active species, Raman spectroscopy, XPS, and XAFS measurements were employed. **Fig. 6** is the Raman spectra of HAp and β-TCP, doped and undoped with Cr. A Raman band at 961 cm^{-1}, which is assignable to HAp (Rath *et al*., 2012), was detected for all HAp-based catalysts (Fig. 6 (A)). Also, Raman bands at 947 and 968 cm^{-1} could be assigned to β-TCP (Cuscó *et al*., 1998) (Fig. 6 (B)). Cr species of Cr-doped catalysts were detected as

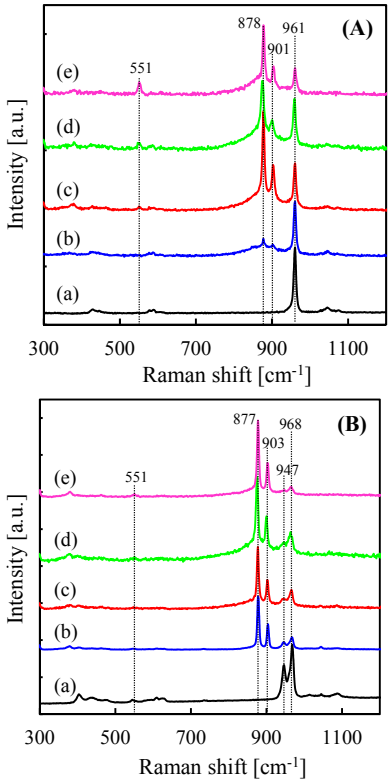

Fig. 6 Raman spectra of (A) (a) HAp(1.67), (b) 1.5 wt% Cr/HAp, (c) 3.5 wt% Cr/HAp, (d) 5.0 wt% Cr/HAp, and (e) 7.0 wt% Cr/HAp, and (B) (a) β-TCP, (b) 1.5 wt% Cr/β-TCP , (c) 3.5 wt% Cr/β-TCP, (d) 5.0 wt% Cr/β-TCP, and (e) 7.0 wt% Cr/β-TCP.

Raman bands centered at 551, 877, 878, 901, and 903 cm^{-1} (Figs. 6 (A) and (B)). According to a previously reported paper (Wang *et al*., 2009), the band at 551 cm^{-1} was attributed to crystalline α-Cr_2O_3 (Wang *et al*., 2009). Also, the bands around 877 and 902 cm^{-1} were assignable to the polychromates of Cr^{6+} species and hydrated chromates, respectively (Hoang *et al*., 2003; Marques *et al*., 2008). As shown in Fig. 6, a Raman band at 551 cm^{-1} gradually increased in both HAp- and β-TCP-based catalysts as the Cr content increased. This tendency was also confirmed in the XRD patterns (Fig. 1).

Fig. 7 shows the XPS spectra of Cr-doped HAp and β-TCP catalysts before and after the ODH of isobutane. This shows that both Cr^{3+} and Cr^{6+} species exist on both catalysts. The standard peak positions for Cr^{3+} and Cr^{6+} species that Boucetta *et al*. (2009) reported were used in the present study. Based on their report, Cr $2p_{3/2}$ and $2p_{1/2}$ due to Cr^{3+} were detected at 577.6 and 587.5 eV, while those due to Cr^{6+} were seen at 589.2 and 579.8 eV, respectively (Fig. 7). After the ODH of isobutane, the peaks shifted to lower binding energies. This result showed that both catalysts were reduced during the reaction and Cr^{3+} species increased. Although differences in the shape of the XPS spectra before and after the reaction were observed, both catalysts showed stable catalytic activities during 6.0 h on-stream. These facts may indicate that the Cr^{3+}, but not the Cr^{6+}, species contributed to the high catalysis for the ODH of isobutane.

XAFS measurement was conducted for Cr-doped samples (**Fig. 8**). In the Cr-*K* edge XANES spectra, a pre-edge peak at ca. 5,991 eV represents tetrahedrally coordinated Cr^{6+} species (Wang *et al*., 2003; Takehira *et al*., 2004). The pre-edge peak of 5.0 wt% Cr/HAp appeared after calcination at 773 K for 3 h, although it disappeared after the ODH of isobutane (Fig. 8 (C)). Similarly, the pre-edge peak of 5.0 wt% Cr/β-TCP disappeared after the ODH of isobutane. These facts reveal that the Cr^{6+} species of Cr-doped catalysts were reduced to Cr^{3+} during the reaction. In the present study, no deactivation of any catalyst was observed during 6.0 h on-stream. Hence, rather than the Cr^{6+} species, the Cr^{3+} species may work as active sites for the ODH of isobutane. Figs. 8 (B) and (D) show the Fourier transformations of the k^3-weighted Cr *K*-edge

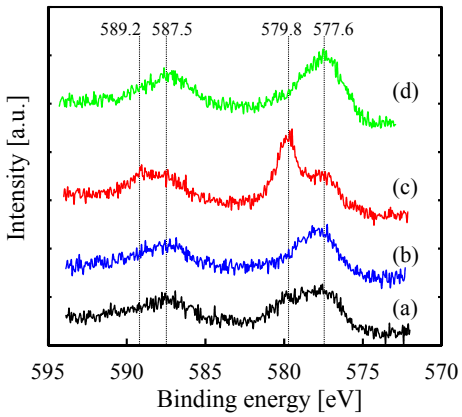

Fig. 7 XPS spectra of 7.0 wt% Cr/HAp (a) before and (b) after the reaction, and 7.0 wt% Cr/β-TCP (c) before and (d) after the reaction.

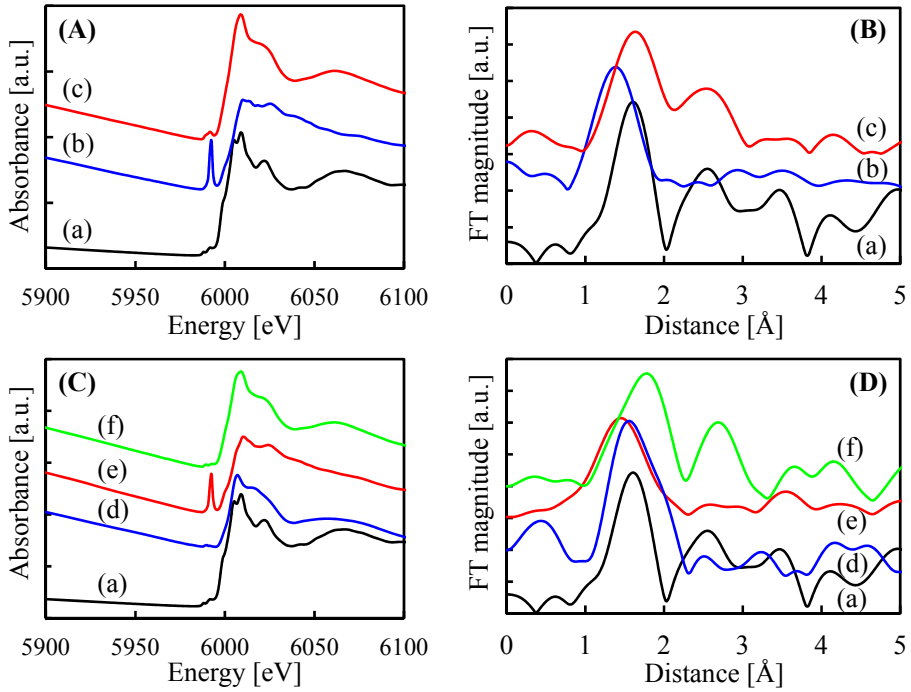

Fig. 8 Cr *K*-edge XANES ((A) and (C)) and Fourier transforms of k^3-weighted EXAFS ((B) and (D)) spectra of (a) α-Cr_2O_3, 5.0 wt% Cr/β-TCP (b) before and (c) after the reaction, (d) uncalcined 5.0 wt% Cr/HAp, 5.0 wt% Cr/HAp (e) before and (f) after the reaction.

EXAFS spectra of crystalline α-Cr_2O_3 (Wako Pure Chemical Industries, Ltd.) and Cr-doped catalysts. Two peaks were observed for α-Cr_2O_3 at 1.60 and 2.55 Å (Figs. 8 (B) and (D)). The Cr^{6+} species of CrO_3, $K_2Cr_2O_7$, and Na_2CrO_4 are known to have CrO_4 tetrahedral coordination with shorter Cr-O bonds observed at 1.20–1.35 Å (Wang *et al.*, 2003). A spectrum of 5.0 wt% Cr/β-TCP (Fig. 8 (B) (b)) at 1.38 Å shifted to 1.62 Å (Fig. 8 (B) (c)) after the reaction. Therefore, it is understandable that the Cr^{6+} species of fresh 5.0 wt% Cr/β-TCP were reduced during the ODH of isobutane. Similar behavior was observed for 5.0 wt% Cr/HAp. A peak of 5.0 wt% Cr/HAp uncalcined at 1.56 Å shifted to 1.44 Å after calcination at 773 K for 3 h (Figs. 8 (D) (d) and (e)). Moreover, the peak at 1.44 Å also shifted to 1.78 Å (Figs. 8 (D) (e) and (f)). In addition to the peak at 1.78 Å, a peak at 2.70 Å was also observed. Although these two peak positions were longer than those of α-Cr_2O_3, these results reveal that the Cr^{6+} species of calcined 5.0 wt% Cr/HAp were reduced during the ODH of isobutane.

2.7 Reducibility of the Cr-doped catalysts

Reducibility of a catalyst is one of the major factors affecting its catalytic activity. **Fig. 9** shows the reducibility of the Cr-doped catalysts with different Cr contents, as evaluated using H_2-TPR. Undoped HAp and β-TCP catalysts showed no reducibility (Figs. 9 (A) (a) and (B) (a)). Also, the reducibility of crystalline α-Cr_2O_3 was evaluated and compared with that of the other catalysts. NH_3- and CO_2-TPD results show that the surface of crystalline α-Cr_2O_3 is almost neutral. Therefore, assuming that crystalline α-Cr_2O_3 can catalyze the ODH of isobutane, it is reasonable to say that its reducibility is the main driving force that catalyzes the ODH of isobutane rather than either its solid acidity or basicity. However, crystalline α-Cr_2O_3 was almost inactive for the ODH of isobutane. Therefore, a higher reducibility than that of crystalline α-Cr_2O_3 would be required to catalyze the ODH of isobutane without catalytic assistance from solid acidity or basicity. A higher reducibility than α-Cr_2O_3 was confirmed for all Cr-doped HAp (Fig. 9 (A)). As the Cr content increased, a reduction peak at approximately 733 K also increased (Fig. 9 (A)). This peak could be attributed to Cr^{3+} species (Santamaría-González *et al.*, 2000). The improvement in the isobutene yield for stoichiometric HAp by the impregnation of Cr was quite limited (Table 5). As stated above, both solid acidity and basicity would be necessary for a high level of activity in stoichiometric HAp(1.67). However, a decrease in the solid acidity of a Cr-doped HAp was also confirmed, as shown in Fig. 5. Therefore, the decrease in solid acidity would lower the original catalytic activity on stoichiometric HAp(1.67). In contrast, newly appearing and high reducibility enhances the catalytic activity. Based on these results, it can be concluded that the combination of improved

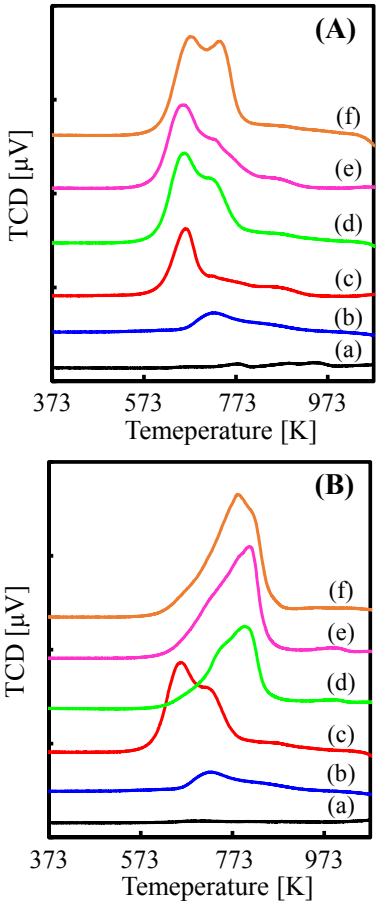

Fig. 9 H_2-TPR spectra of (A) (a) HAp(1.67), (b) α-Cr_2O_3, (c) 1.5 wt% Cr/HAp, (d) 3.5 wt% Cr/HAp, (e) 5.0 wt% Cr/HAp, (f) 7.0 wt% Cr/HAp, (B) (a) β-TCP, (b) α-Cr_2O_3, (c) 1.5 wt% Cr/β-TCP, (d) 3.5 wt% Cr/β-TCP, (e) 5.0 wt% Cr/ β-TCP, and (f) 7.0 wt% Cr/ β-TCP.

reducibility and reduced acidity resulted in a slight increase in the isobutene yield of HAp(1.67) (Table 5).

Fig. 9 (B) shows the H_2-TPR spectra of β-TCP, crystalline α-Cr_2O_3, and Cr-doped β-TCP catalysts. The peak at a lower temperature showed that 1.5 wt% catalyst was more reducible than crystalline α-Cr_2O_3. However, as the Cr content increased, the peak at the lower temperature shifted to a higher temperature. It may be possible that a precursor solution with a higher Cr concentration promoted the aggregation of less-reducible chromium oxides, as confirmed in Figs. 1 and 6. Although the reducibility of 1.5 wt% catalyst was higher than that of more Cr-doped catalysts, the 1.5 wt% Cr-doped β-TCP catalysts showed almost as high catalytic activity as that shown by the other Cr-doped β-TCP catalysts. These results show that a higher reducibility, shown by the peak at 650 K in Fig. 9 (B), was not necessary to catalyze the ODH of isobutane using this catalytic system. The solid basicity of β-TCP may have activated isobutane and assisted less reducible Cr species to catalyze the ODH of isobutane, because the propylene selectivity in the ODH of propane may be

related to the basicity of the Cr^{3+}/HAp system and favors the breaking of the C–H bond of propane along with the formation of propylene (Boucetta *et al*., 2009). Cr species on HAp-based catalysts may be doped near their acidic sites since the reduction in their acidities was confirmed via NH_3-TPD (Fig. 5). Therefore, the original HAp(1.67) is believe to not contribute to the catalytic activities of Cr-doped HAp catalysts since a part of acidic sites that are essential for the catalytic activity of HAp(1.67) would be covered by Cr species. Assuming acidic sites are adjacent to active Cr species on the HAp-based catalysts, the produced isobutene could be adsorbed on an acidic site. In other words, the adsorption could prevent the desorption of isobutene from an acidic site and make the reaction slightly slower. On the contrary, no acidic sites were observed for β-TCP via NH_3-TPD. Hence, the basic surface of β-TCP may have promoted the desorption of isobutene and improved the isobutene selectivity and isobutane conversion.

Conclusions

A stoichiometric HAp showed much greater catalytic activity than β-TCP. However, the catalytic activity of HAp decreased as its Ca/P ratio and basicity decreased. It was possible that both acidic and basic sites on the stoichiometric HAp catalyzed the ODH of isobutane synergistically. The impregnation of Cr improved the catalytic activity of stoichiometric HAp and β-TCP catalysts. Although a stoichiometric HAp showed much greater catalytic activity than β-TCP, the isobutene yield of a Cr-doped (impregnated) HAp was lower than that of a Cr-doped β-TCP. Although the effects of Cr impregnation on the catalytic activity of the stoichiometric HAp appeared to be slight, it may be related to a decrease in its original catalytic activity since its decreased activity was confirmed via NH_3-TPD. The acidity of the stoichiometric HAp may have hindered the immediate desorption of produced isobutene and lowered the isobutene yield of the Cr-doped HAp. Raman spectroscopy, XPS, and XAFS measurements revealed that Cr^{6+} and Cr^{3+} species existed on both Cr-doped HAp and β-TCP. It was confirmed via XPS that the Cr^{6+} species were decreased on both catalysts after the ODH of isobutane. However, both catalysts showed stable catalytic activity during 6.0 h on-stream. This indicated that rather than Cr^{6+}, it was the Cr^{3+} species that contributed to the high catalytic activity during the ODH of isobutane. Also, similar XPS spectra of Cr-doped HAp and β-TCP catalysts after the reaction implied that catalytically active Cr species of both catalysts during the reaction were basically the same.

Acknowledgements

The XAFS study was performed with the approval of the Photon Factory Advisory Committee of the High Energy Research Organization (Proposal 2014G514).

Literature Cited

Angelici, C., M. E. Z. Volthoen, B. M. Weckhuysen and P. C. A. Bruijnincx; "Influence of Acid-Base Properties on the Lebedev Ethanol-to-Butadiene Process Catalyzed by SiO_2–MgO Materials," *Catal. Sci. Technol.*, **5**, 2869–2879 (2015)

Boucetta C., M. Kacimi, A. Ensuque, J.-Y. Piquemal, F. Bozon-Verduraz and M. Ziyad; "Oxidative Dehydrogenation of Propane over Chromium-Loaded Calcium-Hydroxyapatite," *Appl. Catal. A*, **356**, 201–210 (2009)

Cuscó, R., F. Guitián, S.de Aza and L. Artús; "Differentiation between Hydroxyapatite and β-Tricalcium Phosphate by Means of μ-Raman Spectroscopy," *J. Eur. Ceram. Soc.*, **18**, 1301–1305 (1998)

Ehiro, T., A. Itagaki, M. Kurashina, M. Katoh, K. Nakagawa, Y. Katou, W. Ninomiya and S. Sugiyama; "Effect of the Template Ion Exchange Behaviors of Chromium into FSM-16 on the Oxidative Dehydrogenation of Isobutane," *J. Ceramic Soc. Japan*, **123**, 1084–1089 (2015)

Ehiro, T., A. Itagaki, H. Misu, M. Kurashina, K. Nakagawa, M. Katoh, Y. Katou, W. Ninomiya and S. Sugiyama; "Oxidative Dehydrogenation of Isobutane to Isobutene on Metal-Doped MCM-41 Catalysts," *J. Chem. Eng. Japan*, **49**, 136–143 (2016a)

Ehiro, T., A. Itagaki, H. Misu, K. Nakagawa, M. Katoh, Y. Katou, W. Ninomiya and S. Sugiyama; "Effects of Acid Treatment on the Acidic Properties and Catalytic Activity of MCM-41 for the Oxidative Dehydrogenation of Isobutane," *J. Chem. Eng. Japan*, **49**, 152–160 (2016b)

Fajardo, H. V., E. Longo, L. F. D. Probst, A. Valentini, N. L. V. Carreño, M. R. Nunes, A. P. Maciel and E. R. Leite; "Influence of Rare Earth Doping on the Structural and Catalytic Properties of Nanostructured Tin Oxide," *Nanoscale Res. Lett.*, **3**, 194–199 (2008)

Hayek, E. and H. Newsely; "Pentacalcium Monohydroxyorthophosphate (Hydroxyapatite)," *Inorg. Synth.* **7**, 63–65 (1963)

Hoang, D. L., A. Dittmar, J. Radnik, K.-W. Brzezinka and K. Witke; "Redox Behaviour of La-Cr Compounds Formed in CrOx/La_2O_3 Mixed Oxides and CrOx/La_2O_3/ZrO_2 Catalysts," *Appl. Catal. A*, **239**, 95–110 (2003)

Korhonen, S. T., S. M. K. Airaksinen, M. A. Bañares and A. O. I. Krause; "Isobutane Dehydrogenation on Zirconia-, Alumina-, and Zirconia/Alumina-Supported Chromia Catalysts," *Appl. Catal. A*, **333**, 30–41 (2007)

Marques, F. C., M. C. Canela and A. M. Stumbo; "Use of TiO_2/Cr-MCM-41 Molecular Sieve Irradiated with Visible Light for the Degradation of Thiophene in the Gas Phase," *Catal. Today*, **133–135**, 594–599 (2008)

Matsuura, Y., A. Onda, S. Ogo and K. Yanagisawa; "Acrylic Acid Synthesis from Lactic Acid over Hydroxyapatite Catalysts with Various Cations and Anions," *Catal. Today*, **226**, 192–197 (2014)

Ninomiya, W.; "Industrialised Polyoxometalate Catalyst: Heteropolyacid Catalyst for Selective Oxidation of Methacrolein to Methacrylic Acid," *Catal. Catal. (Shokubai)*, **56**, 360–366 (2014)

Ohta, M., Y. Ikeda and A. Igarashi; "Preparation and Characterization of Pt/ZnO-Cr_2O_3 Catalyst for Low-Temperature Dehydrogenation of Isobutane," *Appl. Catal. A*, **258**, 153–158 (2004)

Rath, P. C., L. Besra, B. P. Singh and S. Bhattacharjee; "Titania/Hydroxyapatite Bi-layer Coating on Ti Metal by Electrophoretic Deposition: Characterization and Corrosion Studies," *Ceramics International*, **38**, 3209–3216 (2012)

Santamaría-González, J., J. Mérida-Robles, M. Alcántara-Rodríguez, P. Maireles-Torres, E. Rodríguez-Castellón and A. Jiménez-López; "Catalytic Behaviour of Chromium Supported Mesoporous MCM-41 Silica in the Oxidative Dehydrogenation of Propane," *Catal. Lett.*, **64**, 209–214 (2000)

Sugiyama, S., T. Ehiro, Y. Nitta, A. Itagaki, K. Nakagawa, M. Katoh, Y. Katou, S. Akihara, T. Yasukawa and W. Ninomiya; "Acidic

Properties of Various Silica Catalysts Doped with Chromium for the Oxidative Dehydrogenation of Isobutane to Isobutene," *J. Chem. Eng. Japan*, **48**, 133–140 (2015)

Takehira, K., Y. Ohishi, T. Shishido, T. Kawabata, K. Takaki, Q. Zhang and Y. Wang; "Behavior of Active Sites on Cr-MCM-41 Catalysts during the Dehydrogenation of Propane with CO_2," *J. Catal.*, **224**, 404–416 (2004)

Tsuchida, T., J. Kubo, T. Yoshioka, S. Sakuma, T. Takeguchi and W. Ueda; "Reaction of Ehanol over Hydroxyapatite Affected by Ca/P Ratio of Catalyst," *J. Catal.*, **259**, 183–189 (2008)

Wang, G., L. Zhang, J. Deng, H. Dai, H. He and C. T. Au; "Preparation, Characterization, and Catalytic Activity of Chromia Supported on SBA-15 for the Oxidative Dehydrogenation of Isobutane," *Appl. Catal. A*, **355**, 192–201 (2009)

Wang, Y., Y. Ohishi, T. Shishido, Q. Zhang, W. Yang, Q. Guo, H. Wan and K. Takehira; "Characterizations and Catalytic Properties of Cr-MCM-41 Prepared by Direct Hydrothermal Synthesis and Template-Ion Exchange," *J. Catal*, **220**, 347–357 (2003)

Zhang, L., J. Deng, H. Dai and C. T. Au; "Binary Cr–Mo Oxide Catalysts Supported on MgO-Coated Polyhedral Three-dimensional Mesoporous SBA-16 for the Oxidative Dehydrogenation of *Iso*-butane," *Appl. Catal. A*, **354**, 72–81 (2009)

Zhuang., Z., H. Yamamoto and M. Aizawa; "Synthesis of Plate-Shaped Hydroxyapatite via an Enzyme Reaction of Urea with Urease and its Characterization," *Powder Technol.*, **222**, 193–200 (2012)

Zhuang, Z. and M. Aizawa; "Protein Adsorption on Single-Crystal Hydroxyapatite Particles with Preferred Orientation to a(b)- and c-Axes," *J. Mater. Sci.: Mater. Med.*, **24**, 1211–1216 (2013)